Rate dependence of crack-tip processes predicts twinning trends in f.c.c. metals

D. H. WARNER, W. A. CURTIN* AND S. QU†

Division of Engineering, Brown University, Providence, Rhode Island 02912, USA

†Present address: Institute of Applied Mechanics, College of Mechanical and Energy Engineering, Zhejiang University, Hangzhou, Zhejiang 310027, China

*e-mail: curtin@engin.brown.edu

Published online: 14 October 2007; doi:10.1038/nmat2030

Crack-tip behaviour in metals is among the most basic problems in mechanics of materials. Yet, long-standing experimental evidence suggests that crack-tip twinning in face-centred-cubic (f.c.c.) metals is highly dependent on the material, temperature and loading rate, and previous simulations and models predict twinning in aluminium, where it has never been observed. Here, this discrepancy between theory and experiment is resolved through a new model guided and validated by extensive multiscale simulations. Both the analytic model and simulations reveal a transition from crack-tip twinning at short times to full dislocation formation at long times. Applied to a host of f.c.c. metals, the model agrees with experimental trends as it predicts large differences in the thermal activation needed for full dislocation emission to dominate. More broadly, this work demonstrates the necessity of multiscale modelling and attention to rate dependence for accurate description of material behaviour and computationally guided material design.

Dislocation slip and twinning are important complementary mechanisms for plastic deformation and energy dissipation in many metallic systems. In face-centred-cubic (f.c.c.) materials, twinning and slip occur through dislocation processes operating on the same set of crystallographic slip systems and are thus in direct competition. As shown in Fig. 1a,b, dislocation slip occurs when a leading partial dislocation is followed by a trailing partial dislocation on the same slip plane, creating a full dislocation and leaving no stacking fault. Twinning occurs when a leading partial dislocation is followed by a twinning partial dislocation of the same Burgers vector on the adjacent slip plane, leaving a microtwin boundary (Fig. 1c). Once a microtwin is formed, subsequent partial dislocations of the same character are favoured on adjacent slip planes. As these subsequent twinning partial dislocations nucleate, the twinned region widens and extends outwards as the partials propagate away from the crack tip. The competition between full dislocation emission and twinning at the crack tip influences the nature of crack-tip blunting and thus plays a role in determining ductile (dislocation slip) versus quasi-brittle (twinning) fracture behaviour.

Under ordinary loading conditions at room temperature, deformation twinning and/or crack-tip twinning in f.c.c. metals is typically only observed in Ag (refs 1,2) and Ir (refs 3,4). However, if loading occurs at high rates and/or low temperatures, twinning is ordinarily found in Cu (refs 5–7), Au (ref. 5) and Ni (refs 6,8), but not Al (refs 5,7,9). Although twinning is often claimed to be correlated with low stacking-fault energy, the correlation is not strong. For example, Ir has among the highest stable stacking-fault energies with $\gamma_{ssf} = 480\,\mathrm{mJ\,m^{-2}}$ (ref. 4), whereas Ag has one of the lowest with $\gamma_{ssf} = 21\,\mathrm{mJ\,m^{-2}}$ (ref. 10) and yet both twin fairly readily. A recent criterion for twinnability ranks materials on the basis of the ratio of unstable stacking-fault and unstable twinning-fault energies[10] but predicts that, for a class of ductile orientations, twinning is favourable in all f.c.c. metals studied, including Al. Furthermore, atomistic studies via molecular statics and dynamics on Al show crack-tip twinning[11,12]. There is thus a glaring discrepancy between theory and experiment in this simplest class of materials—pure f.c.c. metals. The inability to properly predict the competition between twinning and dislocation slip, particularly at a crack tip, in such simple materials raises serious questions about the prospects for design of materials as guided by atomistic and nanomechanics computational tools.

Here, we resolve the discrepancy between theory and experiments by considering the thermally activated nature of both twinning and dislocation slip. In general, rate dependence of material behaviour is undergoing a resurgence due to a growing ability to connect macroscopic rate dependence to complex microscopic mechanisms of deformation, with applications to nanocrystalline metals[13,14], dynamic strain ageing[15] and other strengthening mechanisms[16], and so the present work fits within an exciting and broad trend in modern materials science.

We first use a multiscale simulation technique that permits extensive long-time simulations of crack-tip behaviour and shows that in Al there is a transition from twinning at very short times and high applied loads to dislocation slip at longer times and lower applied loads. Twinning in Al is thus very rare, in agreement with experiments. We then extend the two-dimensional (2D) analytic Peierls model of Rice and Beltz[17] to study this competition more generally. The analytic model predicts that, in a wide range of f.c.c. metals, the activation energy for full dislocation emission becomes lower than that for twinning with decreasing load, corresponding to longer times or slower strain rates. The metals differ only in the timescale at which the transition occurs relative to typical experimental times and rates. The ranking of twinnability using this rate criterion matches the observed experimental trends quite well. To elucidate the dependencies on underlying basic material properties, we develop an accurate closed-form expression to predict the activation energy barrier at the crossover from twinning

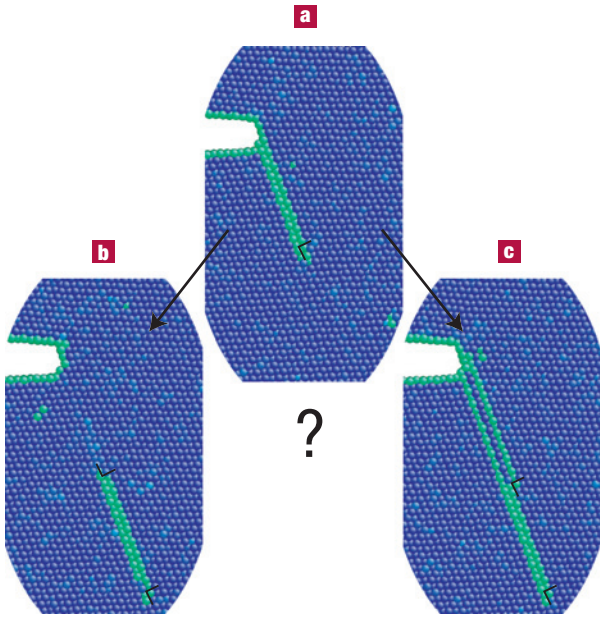

Figure 1 Schematic diagram of two possible modes of crack-tip plasticity in f.c.c. metals. a–c, After the nucleation of the leading partial dislocation (**a**) either full dislocation emission via nucleation of a trailing partial (**b**) or microtwin formation via nucleation of a twinning partial (**c**) can occur. Atoms in perfect f.c.c. packing are coloured blue[37].

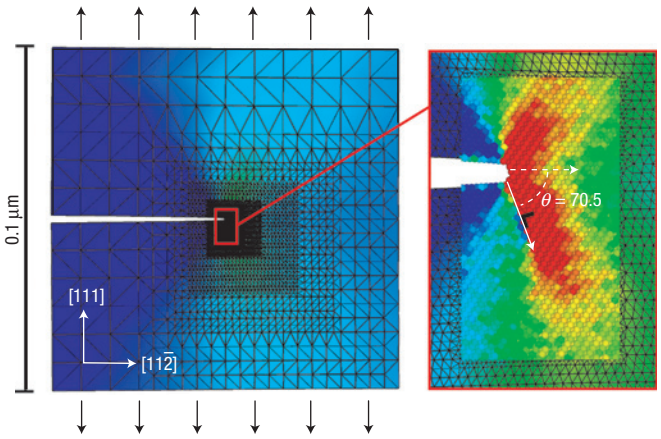

Figure 2 Cross-section of the simulation cell showing the crack and crystal geometry used in this work. The expanded image shows the atomistic resolution at the crack tip after nucleation of the leading partial dislocation. Contours represent strain in the vertical direction.

to full dislocation emission, and this model can serve as a guide for materials design.

To study twinning versus dislocation slip via simulation, a multiscale method is essential in overcoming severe computational hurdles. Because the position of the leading partial dislocation is crucial, standard molecular dynamics approaches[18] would require simulation cell radii of 100 nm to attain an accuracy of 90% in the activation energies. Furthermore, multiple simulations of $t > 10$ ns are required to obtain key results. A direct molecular dynamics approach would thus require thousands of CPU years. Here, we use the finite-temperature concurrent multiscale coupled atomistic discrete dislocation[19] method to minimize the number of explicit atoms in the computational cell without influencing any physical results and reduce the total CPU time to ~11 CPU years. Figure 2 shows a cross-section of the computational cell, after the leading partial dislocation has nucleated on the active slip plane. Second, we use the parallel replica method[20], running many nominally identical simulations on independent CPUs and accumulating total simulation time until the first nucleation event of interest occurs in any one of the simulations. Details are discussed in the Methods section.

With loading fixed at an applied stress intensity K_I, the first event is nucleation of the leading partial dislocation, which then travels to its stable equilibrium position (Fig. 1a). We then measure the further time required for the nucleation of either a trailing (Fig. 1b) or twinning (Fig. 1c) partial dislocation, as shown in Fig. 3. At $T = 300$ K, twin formation dominates at high loads $K_I > 0.185\,\text{eV}\,\text{Å}^{-2.5}$ and very short times $t < 100$ ps. As the load decreases, instances of trailing dislocation nucleation become dominant at the lowest loads and longest times $t > 10$ ns. There is thus a transition from twinning to full dislocation emission with decreasing load or increasing time. Cracks in Al are therefore not predicted to twin at room temperature except under the most extreme conditions of shock loading, consistent with experimental results[5,7,9]. This is the first main result of this article.

We now develop an analytic model to help rationalize and generalize the observed transition from twinning to dislocation slip. The model is an extension of the 2D (plane strain) Peierls model developed by Rice and Beltz[17] for full dislocation nucleation. We compute the total energy of a system containing an initial crack extending from $-\infty$ to 0 along the x direction with slip along a single plane emerging from the crack tip at an angle θ off of the x axis. The total energy includes: the elastic strain energy of the loaded cracked solid without any slip, U_0; the change in atomic stacking energy, Φ, due to a slip discontinuity $\boldsymbol{\delta}(r) = \delta_e(r)\mathbf{e}_{[112]} + \delta_s(r)\mathbf{e}_{[1\bar{1}0]}$, with δ_e and δ_s being the edge and screw components of the slip respectively; the elastic interaction energy between the infinitesimal increments of slip; and the elastic interaction energy between the slip and the crack surface. The total energy is then

$$U[\boldsymbol{\delta}(r)] = U_0 + \int_0^\infty \Phi[\boldsymbol{\delta}(r)]\,\mathrm{d}r + \frac{1}{2}\int_0^\infty \begin{bmatrix} s[\delta_e(r)] \\ (1-\nu)s[\delta_s(r)] \end{bmatrix} \cdot \begin{bmatrix} \delta_e(r) \\ \delta_s(r) \end{bmatrix} \mathrm{d}r - \int_0^\infty \frac{K_{II}^{\text{eff}}}{\sqrt{2\pi r}}\,\mathrm{d}r$$

with

$$s[f(r)] = \frac{\mu}{2\pi(1-\nu)}\int_0^\infty \sqrt{\frac{\xi}{r}}\,\frac{\mathrm{d}f(\xi)/\mathrm{d}\xi}{r-\xi}\,\mathrm{d}\xi,$$

where μ is the material shear modulus, and

$$K_{II}^{\text{eff}} = K_I \cos^2(\theta/2)\sin(\theta/2).$$

Guided by the simulations, the geometry and the Thompson tetrahedron, we constrain the slip paths to pure edge slip in the [112] direction for the leading and twinning partials and mixed edge and screw slip in the [2$\bar{1}$1] direction (or [$\bar{1}$21] equivalent by symmetry) for the trailing partial. The potential Φ is related, but not equal, to the generalized stacking-fault interplanar potential. By approximating the generalized stacking-fault potential to be of Frenkel sinusoidal form along the slip paths,

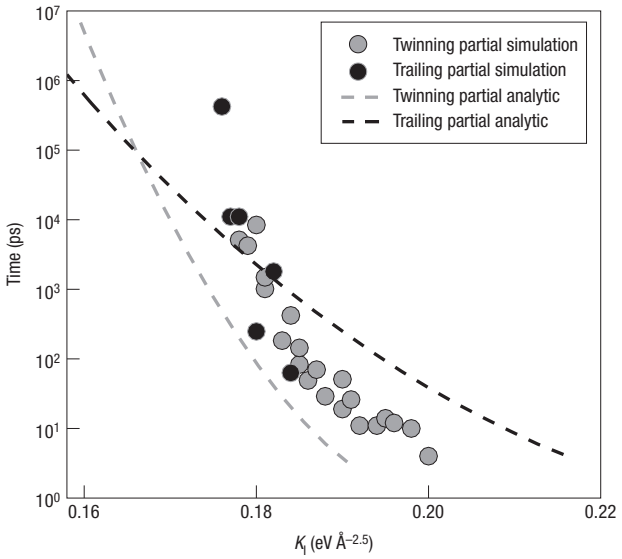

Figure 3 Time to nucleation of a trailing or twinning partial versus applied load in Al at 300 K. Circles: multiscale simulation results. Dashed lines: predictions of the analytic 2D model (equations (1), (2)).

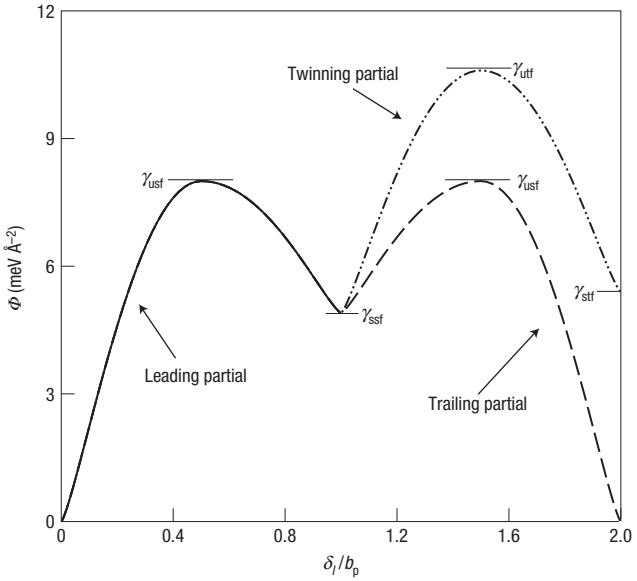

Figure 4 Slip potential Φ along the leading-to-trailing and leading-to-twinning slip paths for Al (ref. 31) at 300 K. δ_l represents the discontinuous slip vector $\boldsymbol{\delta}$ projected onto the slip path. Note the asymmetry in the barrier for emission of the trailing partial.

the calculation of Φ is straightforward[21] and is shown for Al at 300 K in Fig. 4. The extrema of Φ correspond to the various stable and unstable stacking-fault energies (γ_{ssf} and γ_{usf}) and twinning-fault energies (γ_{stf} and γ_{utf}). The activation energy per unit length at any applied load is the difference in energy between the stable equilibrium slip distribution $\boldsymbol{\delta}_{stable}(r)$ and the saddle point slip distribution $\boldsymbol{\delta}_{saddle}(r)$,

$$\Delta U = U[\boldsymbol{\delta}_{saddle}(r)] - U[\boldsymbol{\delta}_{stable}(r)]. \quad (1)$$

Solutions were obtained numerically following the approach of Rice and Beltz[17] but with an adaptive discretization of the slip distribution in the vicinity of the leading partial dislocation to accurately capture its influence on the crack-tip phenomena.

The analytical model, being 2D, yields an activation energy per unit length. To connect with the simulation results requires multiplication by an effective lateral length L of an actual 3D dislocation loop[22] and insertion of the total activation energy $L\Delta U$ into the Arrhenius law

$$\bar{t} = \nu_f^{-1} e^{L\Delta U/kT}, \quad (2)$$

where ν_f is the attempt frequency and k is the Boltzmann factor. Here we use $6 \times 10^{11}\ s^{-1}$, obtained from analysing the rate dependence of the leading partial emission (not shown here). We choose $L = 5b_p \approx 8$ Å, where b_p is the magnitude of the Burgers vector of the nucleated partial dislocations. The length L is roughly consistent with simulation results showing convergence of the nucleation times for leading partial nucleation for simulation cell widths of 12 Å or larger (not shown here). Figure 3 shows the predicted mean nucleation time for both twinning and trailing dislocations versus K_I using equation (1), with material parameters taken from Table 1 at 300 K. The main feature is that the analytic model confirms the transition from twinning to full dislocation slip with decreasing load and increasing time. The model is quantitatively good as well, recognizing the exponential sensitivity of nucleation time to the energy barrier and noting the narrow range of applied loads in the figure. Quantitative disagreement between the model and simulations is in part because the continuum estimate of the zero-temperature stress intensity for nucleation is smaller than the atomistic value, similar to predictions for the emission of the leading partial dislocation[22]. The ability of the model to capture the change in deformation mechanism as found by simulation is the second main result of this article.

We now show that the analytic model further predicts that the mechanism transition is not unique to Al and rationalizes experimental observations of the ability of f.c.c. metals to twin. Table 1 shows the material properties for a range of f.c.c. metals as obtained from various literature sources (see the Methods section). As not all necessary material properties are available, we make the following estimates. First, $\gamma_{stf} \approx \gamma_{ssf}$. Second, we estimate values at 300 K by assuming a scaling $\gamma_{ssf}^{300\,K} = \gamma_{ssf}^{0\,K}(1 - 0.77T/T_m)$ found here for Al (D.H.W., W.A.C., unpublished) and roughly consistent with independent results on Ni (refs 23,24). Third, γ_{usf} and γ_{utf} are assumed to be temperature independent, consistent with our simulations for γ_{usf} (D.H.W., W.A.C., unpublished). With these values, the predicted activation energies per unit length for both twinning and full dislocation slip mechanisms were computed for Ag, Al, Au, Cu, Ir, Ni and Pt as a function of applied stress intensity at 300 K, as shown in Fig. 5. In all cases, there is a crossover from twinning to full dislocation emission as the load is decreased. At zero energy barrier, our analysis is identical to that of Tadmor and Hai[10] and predicts that all of these f.c.c. materials twin at $T = 0$ K or extremely high rates of loading. The occurrence of the full dislocation slip mechanism is entirely due to thermal activation rate effects, missing in previous analyses but crucial to a proper understanding of the material behaviour.

The predicted activation energy per unit length at the transition from twinning to full dislocation emission is shown in Table 1. The data reveal that extremely high strain rates or loads are necessary for twin nucleation in Al, Pt and Au, whereas crack-tip twinning would regularly occur under typical experimental conditions in Ag, Cu and Ir for this geometry. These predictions show a strong

Table 1 Material parameters at 300 K used to examine the transition from twinning to full dislocation emission in various f.c.c. metals. The values for the material parameters are discussed in the Methods section. ΔU_{trans}, the numerically computed activation energy per unit length at the transition point, and $\Delta U_{trans}^{approx}$, a closed-form approximation of the activation energy at the transition (equation (5)), are also shown. The transition time represents the expected time at which full dislocation nucleation is favoured over twinning at room temperature, computed as $\bar{t} = \nu_f^{-1} e^{L\Delta U/kT}$ where $\nu_f = 6 \times 10^{11}\ s^{-1}$, $kT = 0.0258$ eV and $L = 5b_p$.

Material	b_p (Å)	μ (GPa)	ν	γ_{usf} (J m^{-2})	γ_{ssf} (J m^{-2})	γ_{utf} (J m^{-2})	γ_{stf} (J m^{-2})	ΔU_{trans} (eV Å^{-1})	$\Delta U_{trans}^{approx}$ (eV Å^{-1})	Transition time
Al	1.65	29.2	0.319	0.128	0.079	0.168	0.087	0.034	0.031	micro-seconds
Pt	1.60	65.2	0.393	0.388	0.240	0.522	0.240	0.058	0.049	micro-seconds
Au	1.66	30.9	0.416	0.110	0.040	0.135	0.040	0.066	0.058	micro-seconds
Ni	1.44	93.2	0.285	0.173	0.104	0.236	0.104	0.089	0.075	seconds
Ag	1.67	56.7	0.354	0.093	0.018	0.106	0.014	0.113	0.101	hours
Cu	1.48	54.8	0.325	0.200	0.053	0.236	0.053	0.127	0.115	hours
Ir	1.57	221.6	0.242	0.679	0.280	0.872	0.280	0.442	0.436	≫ giga-years

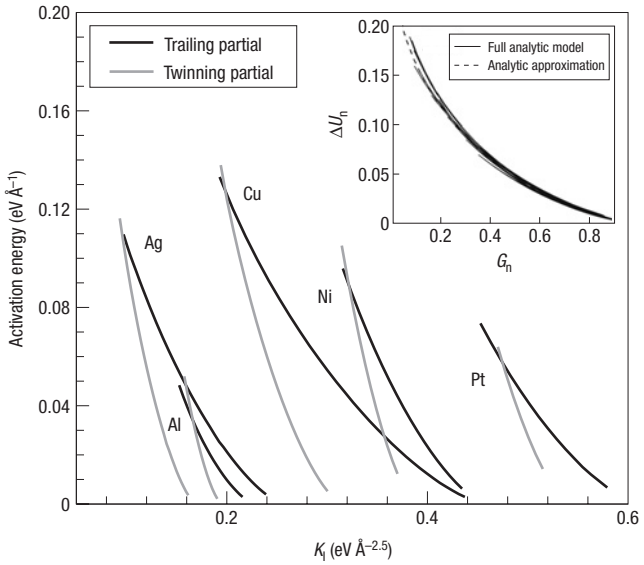

Figure 5 Activation energy per unit length versus applied load for both twinning and trailing partial emission for a range of f.c.c. metals. Lines computed with the 2D analytic model at 300 K (equation (1)). Note the crossover to lower energy for trailing partial emission at lower loads and higher activation energies. Inset: Normalized activation energy ΔU_n at the twinning/trailing transition versus normalized applied load, for both full analytic model (solid lines) and the closed-from analytic approximation (equation (5); dashed line), showing excellent agreement for all materials examined in this work. The normalization is $\Delta U_n = \Delta U/A$ and $G_n = (G - C)/B$, where A, B and C come from expressing equations (3) and (4) in the form $\Delta U = A(1 - \sqrt{(G - C)/B})^{3/2}$.

correlation with the experimental observations as described earlier. Nevertheless, there is not one-to-one correspondence as Ni is predicted to twin slightly more readily than Au. Such differences are not surprising considering that the analytic model is 2D with some simplifications, the temperature dependence of the input material parameters has some uncertainty, the appropriate length parameter L that determines actual rates is probably material dependent and that the deformation in the cited experiments could be the result of more complex deformation mechanisms in addition to dislocation nucleation[2].

Despite the broad success of the analytic model, its application requires extensive computations and does not bring out basic material dependencies. We have thus developed a comparatively simple formula that is quantitatively accurate while clearly showing material dependencies. We start with the asymptotic simplification given by Rice and Beltz[17] and adjust for the emission of mixed-character dislocations, the shielding of the stress intensity factor at the crack tip by the leading partial and the annihilation/creation of stable stacking/twinning faults, all depending on which case of partial nucleation is being considered. For the current geometry, the activation energy for the twinning partial can then be expressed as

$$\Delta U \approx \frac{0.287\mu b_p^2\left(1 - \frac{\gamma_{ssf} - \gamma_{stf}}{2\gamma_{utf}}\right)}{(1-\nu)}\left(1 - \sqrt{\frac{G - \gamma_{ssf}}{(\gamma_{utf} - \gamma_{ssf})}}\right)^{3/2} \quad (3)$$

and for the trailing partial as

$$\Delta U \approx \frac{0.287\mu b_p^2\left(1 - \frac{\gamma_{ssf}}{2\gamma_{usf}}\right)}{(1-\frac{\nu}{4})}\left(1 - \sqrt{\frac{G - \gamma_{ssf}}{(\gamma_{usf} - \gamma_{ssf})(4-3\nu)}}\right)^{3/2} \quad (4)$$

where $G = (1-\nu)K_{eff}^2/2\mu$. The accuracy of equations (3) and (4) is shown in the inset of Fig. 5 where all materials examined have effectively been collapsed onto a single line by appropriate normalization of the axes. By equating the activation energies in equations (3) and (4), we can solve for G at the transition point and then for the activation energy at the transition point, to obtain

$$\Delta U_{trans} \approx \Delta U_{trans}^{approx} = \frac{0.287\mu b_p^2\left(1 - \frac{\gamma_{ssf} - \gamma_{stf}}{2\gamma_{utf}}\right)}{1-\nu} \times \left(1 - \frac{\lambda - 1}{\lambda - \sqrt{\frac{\gamma_{utf} - \gamma_{ssf}}{(\gamma_{usf} - \gamma_{ssf})(4-3\nu)}}}\right)^{3/2} \quad (5)$$

with

$$\lambda = \left(\frac{4-\nu}{4(1-\nu)}\frac{\left(1 - \frac{\gamma_{ssf} - \gamma_{stf}}{2\gamma_{utf}}\right)}{\left(1 - \frac{\gamma_{ssf}}{2\gamma_{usf}}\right)}\right)^{2/3}.$$

The values predicted by equation (5) are labelled as $\Delta U_{trans}^{approx}$ in Table 1, and show very good agreement with the full numerical values ΔU_{trans}.

Using equation (5), we can now examine the predicted trends for the twinning versus slip transition as a function of material properties. An immediate conclusion from equation (5) is that ΔU_{trans} is proportional to both the Burgers vector and the shear

modulus. The various fault energies influence ΔU_{trans} through various interdependent ratios that reduce to two ratios if $\gamma_{ssf} \approx \gamma_{stf}$. First, increasing the ratio $\gamma_{ssf}/\gamma_{usf}$ decreases ΔU_{trans}, making twinning less likely, by decreasing the stress dependence of the activation energy of the trailing partial. The stress dependence is lower because the trailing partial eliminates the stacking fault on the activated side of the energy barrier, that is, for slips $\delta_l > 3b_p/2$ (Fig. 4), to yield less total slip at the saddle point and thus a lower saddle-state energy. Second, decreasing the ratio $\gamma_{utf} - \gamma_{ssf}/\gamma_{usf} - \gamma_{ssf}$ decreases ΔU_{trans} and makes twinning less likely. This quantity is the ratio between the excess atomic stacking energies required at the crack tip for the twinning and trailing cases (Fig. 4) and is the determining factor in the (non-activated) limit $\Delta U \to 0$. It therefore establishes the difference between the $T = 0$ stress intensities for nucleation of twinning and trailing seen in Fig. 5. As the $T = 0$ difference becomes smaller, the crossover from twinning to full dislocation deformation can occur at lower activation energies.

Although the current analysis of crack-tip twinning does not directly apply to twinning in the interior of traditional polycrystalline metals[2], it is probably extendable to nanocrystalline metals where dislocation nucleation from grain boundaries plays a key role in the deformation[25,26]. In nanocrystalline metals in a particular range of grain sizes, atomistic simulations exhibit deformation by exclusive emission of leading partial dislocations on non-adjacent slip planes[27] resulting in the formation of large numbers of stacking faults, an observation not supported by experiments[28]. The resolution of this discrepancy may lie in the rate dependence of trailing partial nucleation, analogous to that proposed here for crack-tip deformation. At lower loading rates or longer times, simulations might show a transition from exclusive leading partial emission to either twinning or full dislocation emission as seen experimentally. Such a nucleation process would differ in detail from the problem modelled here (owing to factors such as the nature of the local stress concentration that drive emission from the grain boundary, lower image stresses on emitted partials, differences in stress gradients that control the position of the leading partial dislocation and the absence of a free surface for accommodation of the slip steps) but bears qualitative similarities to the present modelling.

In summary, we have used multiscale simulations and analytic models to demonstrate a transition in the mechanical behaviour of metals—from twinning to dislocation slip—that is fundamentally atomistic in nature but not computationally accessible by standard atomistic methods. Our analyses reveal that the competition between the two mechanisms is strongly rate dependent, with dislocation slip preferable at lower loads and/or lower loading rates. This finding rationalizes the long-established metallurgical wisdom that deformation twinning is most likely when deformation occurs at high rates and low temperatures. Specific predictions for a range of f.c.c. metals are largely consistent with the available data and a simple formula brings out the major factors controlling the competing deformation mechanisms and the transition between them. More generally, this work demonstrates that multiscale methods and rate dependence are not just desirable but can be essential in pursuing the proper prediction of material behaviour, and are thus key components in the thrust for designing materials using computational materials science.

METHODS

The simulations were conducted at 300 K on single-crystal Al containing an initial crack orientation such that dislocation emission would occur along a slip plane oriented at $\theta = 70.5°$ from the crack plane on plane-strain mode I loading. The specific crystallography corresponds to the (111) plane coinciding with the crack plane and the crack tip being parallel to the $[\bar{1}10]$ direction as shown in Fig. 2. This geometry is the most favourable for twin emission under mode I loading and thus provides a limiting bound for the occurrence of thermally activated crack-tip twinning[10,29]. The dimensions of the system were $0.2 \times 0.2 \times 0.002\,\mu m$, simulated using only 23,423 degrees of freedom: 15,141 atoms in a fully 3D atomistic region ($84 \times 147 \times 20$ Å) surrounded by 8,282 finite-element nodes in a plane-strain linear elastic region. The lateral size of the atomistic region was varied to confirm that no artefacts were introduced by the presence of the atomistic/continuum interface. In the through-thickness z direction, converged results for all sizes above 12 Å were obtained, consistent with previous molecular dynamics studies on nucleation of leading partial dislocations[30]. The Ercolessi–Adams embedded atom method (EAM) potential was used to describe the Al interatomic interactions[31].

Loading was controlled by application of displacements to the outer boundaries of the specimen corresponding to the anisotropic elastic mode I stress intensity factor, K_I, from the continuum solution for a sharp crack[32]. The initial displacements throughout the sample were obtained from the same analytic fields.

For fixed loads greater than 0.182 eV $Å^{-2.5}$, standard single-processor calculations were carried out. For lower loads, each calculation was computed from the sum of parallel replicas. Thus, multiple simulations that varied only in the initial random velocities were simultaneously carried out on multiple processors. When the first instance of nucleation occurred on any processor, all simulations were stopped and the time of the nucleation event was considered to be the sum of the simulation time on all of the processors.

The material parameters used in the analytic analysis and shown in Table 1 were obtained as follows. For Al, the fault energies are derived from the EAM potential of Ercolessi and Adams[31] as measured by Tadmor and Hai[10] at 0 K. For Ni, the energies are derived from the EAM potential of Mishin *et al.*[33] as measured by Van Swygenhoven *et al.*[28] at 0 K. For all of the other metals, the energies are derived from the tight-binding calculations of Tadmor and Bernstein[29,34] at 0 K. The extrapolation of the energies from 0 to 300 K is described in the main text. With the exception of Al, the finite-temperature isotropic elastic constants were obtained from the CRC handbook[35] using a Voigt average[36].

Received 11 April 2007; accepted 7 September 2007; published 14 October 2007.

References

1. English, A. T. & Chin, G. Y. On the variation of wire texture with stacking fault energy in f.c.c. metals and alloys. *Acta Metall.* **13**, 1013–1016 (1965).
2. Venables, J. in *Proc. of the Mettallurgical Society Conference* Vol. 25 (ed. Reed-Hill, R.) 77–111 (Gordon and Breach Science, New York, 1963).
3. Adamesku, R., Grebenkin, S., Yermaakov, A. & Panfilov, P. On mechanical twinning in iridium under compression at room temperature. *J. Mater. Sci. Lett.* **13**, 865–867 (1994).
4. Fortes, M. & Ralph, B. Deformation twinning and double twinning in iridium. *J. Less-Common Met.* **22**, 201–208 (1970).
5. Blewitt, T. H., Coltman, R. R. & Redman, J. K. Low-temperature deformation of copper single crystals. *J. Appl. Phys.* **28**, 651–660 (1957).
6. Murr, L. & Esquivel, E. Observations of common microstructural issues associated with dynamic deformation phenomena: Twins, microbands, grain size effects, shear bands, and dynamic recrystallization. *J. Mater. Sci.* **39**, 1153–1168 (2004).
7. Thornton, P. & Mitchell, T. Deformation twinning in alloys at low temperatures. *Phil. Mag.* **7**, 361–375 (1962).
8. Haasen, P. Plastic deformation of nickel single crystals at low temperatures. *Phil. Mag.* **3**, 384–418 (1958).
9. Gray, G. I. & Huang, J. Influence of repeated shock loading on the substructure evolution of 99. 99 wt. percent aluminum. *Mater. Sci. Eng. A* **145**, 21–35 (1991).
10. Tadmor, E. & Hai, S. A Peierls criterion for the onset of deformation twinning at a crack tip. *J. Mech. Phys. Solids* **51**, 765–793 (2003).
11. Farkas, D., Duranduru, M., Curtin, W. A. & Ribbens, C. Multiple-dislocation emission from the crack tip in the ductile fracture of Al. *Phil. Mag. A* **81**, 1241–1255 (2001).
12. Hai, S. & Tadmor, E. B. Deformation twinning at aluminum crack tips. *Acta Mater.* **51**, 117–131 (2003).
13. Van Swygenhoven, H., Derlet, P. & Froseth, A. Nucleation and propagation of dislocations in nanocrystalline fcc metals. *Acta Mater.* **54**, 1975–1983 (2006).
14. Zhu, T., Li, J., Samanta, A., Kim, H. G. & Suresh, S. Interfacial plasticity governs strain rate sensitivity and ductility in nanostructured metals. *Proc. Natl Acad. Sci.* **104**, 3031–3036 (2007).
15. Curtin, W. A., Olmsted, D. L. & Hector, L. G. A predictive mechanism for dynamic strain ageing in aluminium–magnesium alloys. *Nature Mater.* **5**, 875–880 (2006).
16. Caillard, D. & Martin, J. *Thermally Activated Mechanisms in Crystal Plasticity* (Pergamon Materials Series, Elsevier, Oxford, 2003).
17. Rice, J. R. & Beltz, G. E. Activation energy for dislocation nucleation at a crack. *J. Mech. Phys. Solids* **42**, 333–360 (1994).
18. Hess, B., Thijsse, B. J. & Van der Giessen, E. Molecular dynamics study of dislocation nucleation from a crack tip. *Phys. Rev. B* **71**, 054111 (2005).
19. Qu, S., Shastry, V., Curtin, W. A. & Miller, R. E. A finite-temperature dynamic coupled atomistic/discrete dislocation method. *Model. Simul. Mater. Sci. Eng.* **13**, 1101–1118 (2005).
20. Voter, A. F. Parallel replica method for dynamics of infrequent events. *Phys. Rev. B* **57**, R13985–R13988 (1998).

21. Rice, J. Dislocation nucleation from a crack tip. An analysis based on the Peierls concept. *J. Mech. Phys. Solids* **40**, 239–271 (1992).
22. Zhu, T., Li, J. & Yip, S. Atomistic study of dislocation loop emission from a crack tip. *Phys. Rev. Lett.* **93**, 025503 (2004).
23. Hasnaoui, A., Van Swygenhoven, H. & Derlet, P. M. Cooperative processes during plastic deformation in nanocrystalline fcc metals: A molecular dynamics simulation. *Phys. Rev. B* **66**, 184112 (2002).
24. Meyer, R. & Lewis, L. J. Stacking-fault energies for Ag, Cu, and Ni from empirical tight-binding potentials. *Phys. Rev. B* **66**, 052106 (2002).
25. Asaro, R. J. & Suresh, S. Mechanistic models for the activation volume and rate sensitivity in metals with nanocrystalline grains and nano-scale twins. *Acta Mater.* **53**, 3369–3382 (2005).
26. Kumar, K., Van Swygenhoven, H. & Suresh, S. Mechanical behavior of nanocrystalline metals and alloys. *Acta Mater.* **51**, 5743–5774 (2003).
27. Yamakov, V., Wolf, D., Phillpot, S. R., Mukherjee, A. K. & Gleiter, H. Deformation-mechanism map for nanocrystalline metals by molecular-dynamics simulation. *Nature Mater.* **3**, 43–47 (2004).
28. Van Swygenhoven, H., Derlet, P. & Froseth, A. Stacking fault energies and slip in nanocrystalline metals. *Nature Mater.* **3**, 399–403 (2004).
29. Tadmor, E. B. & Bernstein, N. A first-principles measure for the twinnability of FCC metals. *J. Mech. Phys. Solids* **52**, 2507–2519 (2004).
30. Horstemeyer, M., Baskes, M. & Plimpton, S. Computational nanoscale plasticity simulations using embedded atom potentials. *Theory Appl. Fract. Mech.* **37**, 49–98 (2001).
31. Ercolessi, F. & Adams, J. B. Interatomic potentials from 1st-principles calculations—the force-matching method. *Europhys. Lett.* **26**, 583–588 (1994).
32. Sih, G., Paris, P. & Irwin, G. R. On cracks in rectilinearly anisotropic bodies. *Int. J. Fract. Mech.* **1**, 189–203 (1965).
33. Mishin, Y., Farkas, D., Mehl, M. J. & Papaconstantopoulos, D. A. Interatomic potentials for monoatomic metals from experimental data and ab initio calculations. *Phys. Rev. B* **59**, 3393–3407 (1999).
34. Bernstein, N. & Tadmor, E. B. Tight-binding calculations of stacking energies and twinnability in fcc metals. *Phys. Rev. B* **69**, 094116 (2004).
35. Lide, D. (ed.) *CRC Handbook of Chemistry and Physics* 82nd edn (CRC Press, New York, 2001).
36. Hirth, J. & Lothe, J. *Theory of Dislocations* (McGraw-Hill, New York, 1968).
37. Li, J. AtomEye: An efficient atomistic configuration viewer. *Model. Simul. Mater. Sci. Eng.* **11**, 173–177 (2003).

Acknowledgements

This work was supported by the Office of Naval Research, Materials Research Division, through Grant No. N00014-05-1-0705.
Correspondence and requests for materials should be addressed to W.A.C.

Rate dependence of crack-tip processes predicts twinning trends in f.c.c. metals

D. H. WARNER, W. A. CURTIN AND S. QU

Nature Materials **6**, 876–881 (2007).

The authors wish to make a correction to the first equation in this Article. They had omitted $\delta_e(r)$ from the final term. The correct equation is:

$$U[\boldsymbol{\delta}(r)] = U_0 + \int_0^\infty \Phi[\boldsymbol{\delta}(r)]\mathrm{d}r + \frac{1}{2}\int_0^\infty \begin{bmatrix} s[\delta_e(r)] \\ (1-\nu)\,s[\delta_s(r)] \end{bmatrix} \cdot \begin{bmatrix} \delta_e(r) \\ \delta_s(r) \end{bmatrix} \mathrm{d}r - \int_0^\infty \frac{K_{II}^{eff}}{\sqrt{2\pi r}}\,\delta_e(r)\mathrm{d}r$$